

# The Effects of Observed Fractional Vegetation Cover on the Land Surface Climatology of the Community Land Model

MICHAEL BARLAGE AND XUBIN ZENG

*Institute of Atmospheric Physics, The University of Arizona, Tucson, Arizona*

(Manuscript received 3 October 2003, in final form 19 April 2004)

## ABSTRACT

Accurate modeling of surface processes requires a specification of the amount of land covered by vegetation. The National Center for Atmospheric Research Community Land Model (CLM2) does not realistically represent sparsely vegetated regions because of a lack of bare soil in the model. In this study, the existing CLM2 surface dataset is replaced by a global 1-km fractional vegetation cover dataset. This results in a doubling of global bare soil fraction in the model. It also significantly affects the fractional coverages of shrub, grass, and crop compared with only minor changes to trees. Regional changes occur most greatly in Australia, with an increase of over 0.4 in bare soil fraction. The western United States, southern South America, and southern Africa show fractional increases of more than 0.2. Simulations of CLM2 coupled with the Community Atmosphere Model (CAM2) show several regions with statistically significant decreases of up to 2 K in 2-m air temperature and up to 10 K in ground temperature, which reduces the high temperature bias in arid and semiarid regions in the model. In Australia, the vegetation changes result in an increase in net downward longwave radiation, which is balanced by an increase of latent and sensible heat fluxes and a decrease of absorbed solar radiation.

## 1. Introduction

The Community Land Model (CLM2; Bonan et al. 2002b) is the land surface component in the National Center for Atmospheric Research (NCAR) Community Climate System Model (CCSM2). CLM2 is an ever-evolving land surface model built by a multi-institutional effort that also produced its predecessor, the Common Land Model (Zeng et al. 2002; Dai et al. 2003). CLM2 requires several parameters to accurately describe the morphology of the vegetated surface.

Fractional vegetation cover (FVC) is an important prescribed parameter in land surface modeling. Roughly 30% of the earth's surface is covered by land. The amount of the land surface that is covered with plants is vital to an accurate simulation of the climate system. Therefore, FVC is crucial for correctly simulating the momentum, water, energy, and trace gas transfers between the land surface and the atmosphere.

The main deficiency of the FVC dataset used in the CCSM2 is the lack of bare soil in sparsely vegetated areas. For instance, the bare soil fraction is erroneously specified as zero over the arid southwestern United States. The purpose of this paper is to replace the existing CCSM2 dataset (Bonan et al. 2002a) by the global

1-km FVC data from Zeng et al. (2000) and to evaluate its impact on the land surface climatology of the CLM2 coupled with the Community Atmosphere Model (CAM2), which is the atmosphere component of CCSM2. Section 2 briefly describes the methodology of introducing the FVC changes into CLM2. Section 3 discusses the results, while the conclusions are given in section 4.

## 2. Methodology

The vegetation amount in CLM2 is represented by spatially variable and season-independent FVC and the spatially and temporally variable leaf area index (LAI). Therefore, a change in the vegetated surface fraction requires a change of the LAI to maintain the same vegetation amount.

### a. New plant functional type dataset

Land cover in CLM2 is represented as a mosaic of five possible land cover types: lake, wetland, urban, glacier, and vegetation, which is then distributed into a maximum of four plant functional types (PFTs). For the hypothetical example given in Fig. 1, the fractional cover of each PFT patch is with respect to the 40% vegetated area of the grid box. For instance, of the 40% that is vegetated, 37% (14.8% of the total grid cell) is broadleaf deciduous tree from a temperate climate.

The creation of the global PFT coverage currently in

---

*Corresponding author address:* Michael Barlage, Institute of Atmospheric Physics, The University of Arizona, 1118 E. 4th St., Tucson, AZ 85721.  
E-mail: barlage@atmo.arizona.edu

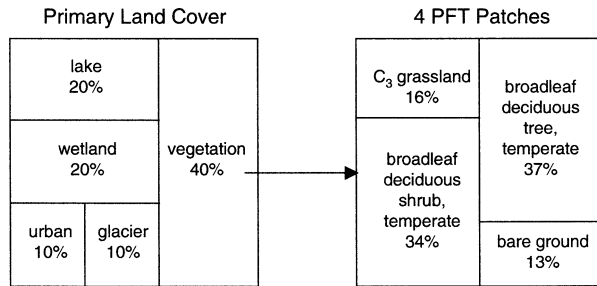


FIG. 1. The mosaic representation of land in CLM2 for a hypothetical grid cell. The cell is comprised of five different land types and four different plant functional types, one of which can be bare ground (after Fig. 1 of Bonan et al. 2002a).

CLM2 is based on the 1-km datasets of International Geosphere–Biosphere Programme (IGBP) natural and anthropogenic land cover (Loveland et al. 2000) and University of Maryland (UMD) tree cover (DeFries et al. 1999, 2000). These datasets are used initially to determine the percentages of seven primary PFTs: needleleaf evergreen tree, needleleaf deciduous tree, broadleaf evergreen tree, broadleaf deciduous tree, shrub, grass, and crop. The resolution of the primary PFT dataset is reduced to  $0.5^\circ$  by finding the latitude and longitude of each 1-km grid cell and averaging the 1-km coverages in each  $0.5^\circ$  grid cell. The seven primary PFTs are then expanded to 15 final physiological variants based on a set of climate rules (see Bonan et al. 2002a). The surface temperature and precipitation climatology at  $0.5^\circ$  resolution compiled by Legates and Willmott (1990a,b) are used. The resulting 15 PFTs along with the barren land category are shown in Table 1.

As mentioned earlier, the current surface cover generation methodology for CLM2 produces too little bare soil in sparsely vegetated areas. This method for generating the  $0.5^\circ$  dataset produces bare soil only if bare soil is the dominant IGBP land cover type on a 1-km grid cell. The final PFT coverage for the global model grid will contain bare soil only if it is one of the four most prevalent types in the  $0.5^\circ$  dataset. In arid shrub-covered regions, a grid cell will be classified as shrub even though substantial bare soil patches can exist between individual shrubs. This method results in zero bare soil fraction over the arid southwestern United States even though substantial interplant bare soil exists (see Zeng et al. 2000). Here, the 1-km FVC dataset of Zeng et al. (2000) is used to enhance the current PFT coverage map.

The FVC dataset was generated using global 1-km Normalized Difference Vegetation Index (NDVI) data. For each 1-km grid cell, the annual maximum NDVI data ( $N_{\max}$ ) are obtained, and the  $N_{\max}$  data are binned by IGBP land cover type. This  $N_{\max}$  histogram is used to determine a critical value ( $N_c$ ) for each IGBP land type that corresponds to full canopy cover. The FVC in each 1-km grid cell is then found by taking the ratio of ( $N_{\max} - N_s$ ) for the grid cell to ( $N_c - N_s$ ) for the cell's

TABLE 1. The plant functional types represented in CLM2 and their fraction of global coverage in the current and new global map.

Plant functional type		Current	New
0	Barren	0.174	0.352
1	Evergreen needleleaf temperate tree	0.031	0.028
2	Evergreen needleleaf boreal tree	0.042	0.038
3	Deciduous needleleaf boreal tree	0.012	0.011
4	Evergreen broadleaf tropical tree	0.057	0.056
5	Evergreen broadleaf temperate tree	0.009	0.009
6	Deciduous broadleaf tropical tree	0.037	0.033
7	Deciduous broadleaf temperate tree	0.025	0.021
8	Deciduous broadleaf boreal tree	0.005	0.004
9	Evergreen broadleaf shrub	0.002	0.001
10	Deciduous broadleaf temperate shrub	0.090	0.030
11	Deciduous broadleaf boreal shrub	0.071	0.046
12	$C_3$ arctic grass	0.075	0.059
13	$C_3$ nonarctic grass	0.134	0.110
14	$C_4$ grass	0.074	0.059
15	Crop	0.163	0.142

IGBP type, with  $N_s$  being the NDVI for bare soil. More details and validation can be found in Zeng et al. (2000). Currently, we are deriving the FVC data based on Moderate Resolution Imaging Spectroradiometer (MODIS) data. Preliminary computation shows that the difference between the MODIS and NDVI FVC data of Zeng et al. (2000) is much smaller than the difference between the data of Zeng et al. (2000) and those used in CLM2.

A similar approach to Bonan et al. (2002a) is used to determine a new PFT coverage, except that FVC is considered in the 1-km calculation of the seven primary PFTs. A flowchart of the procedure is shown in Fig. 2. For each 1-km grid cell, the FVC dataset of Zeng et al. (2000) is used to determine the amount of bare soil at the surface. Next, the 1-km tree cover dataset (DeFries et al. 2000) is used to determine the fraction of trees in the nonbare portion of the grid cell with the remaining fraction determined by the IGBP land cover dataset

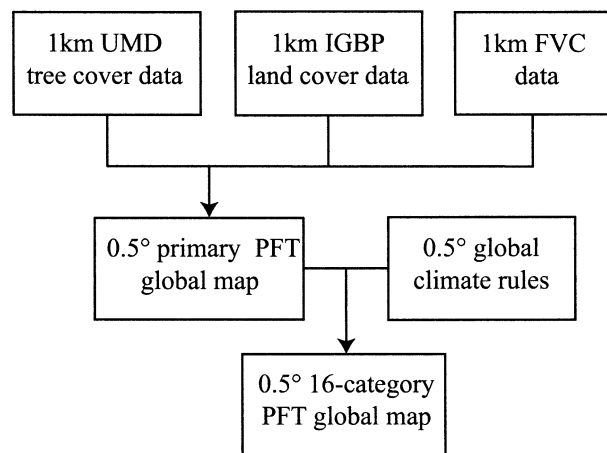


FIG. 2. Flowchart for the creation of the global  $0.5^\circ$  PFT coverage. UMD tree cover, IGBP land cover, and FVC at 1-km resolution are combined to form a  $0.5^\circ$  global map of primary PFTs that are then converted into a global map of the 15 final PFTs (plus bare soil) by combination with Legates and Willmott (1990a,b) climate rules.

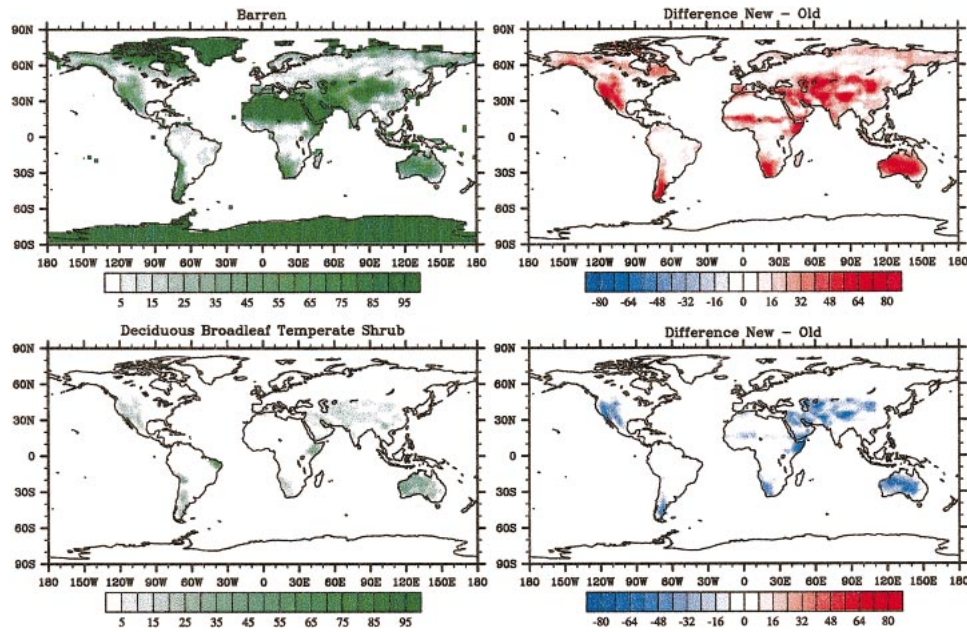


FIG. 3. (left) The percentage of each T42 resolution grid cell that contains (top) bare soil or (bottom) deciduous broadleaf temperate shrub using the FVC data and (right) the difference of percentage coverage between the new vs old PFT datasets.

(Loveland et al. 2000). The 1-km primary PFT coverage dataset is then averaged to a  $0.5^\circ$  grid and combined with the Legates and Willmott (1990a,b) temperature and precipitation climatology to produce the final  $0.5^\circ$  PFT dataset.

#### b. Changes introduced by the new PFT method

When the new dataset in section 2a is applied to the CAM2/CLM2 system at T42 resolution, the changes to bare soil and the deciduous broadleaf temperate shrub PFT (PFTs 0 and 10 in Table 1) are shown in Fig. 3. Many of the large changes from the current land surface representation (upper right) occur in sparsely vegetated regions such as the southwestern United States, southern South America, southern Africa, and central Australia. Regions with large tree coverage are not affected by the new method because of the large fractional coverage of most tree-covered regions (see Table 1 of Zeng et al. 2000). Regions with no vegetation, like the Sahara Desert, cannot be affected either by the new method.

Some of the regions with greatest PFT change correspond to regions where Bonan et al. (2002b) compared the surface energy budget, temperature, precipitation, and runoff for several global land regions. The PFT changes introduced by the new surface cover method and latitude and longitude ranges for these regions are shown in Table 2. Most regions, especially regions predominately covered with shrubs or grasses, show a substantial increase in bare soil fraction. For example, the western United States, southern South America, and southern Africa show increases of more than 0.2 in bare

soil fraction. Australia is most greatly affected, with an increase of over 0.4 in bare soil coverage. India shows a surprising increase in bare soil fraction because this region's boundary includes the northern mountainous areas that have large shrub coverage (see Fig. 3). Densely tree-covered regions, such as the Amazon, the Congo, and Central America, show only small increases in bare soil, as expected. Even less densely tree-covered regions in temperate climates, such as the eastern United States, show only minor increases in bare soil fraction.

The fractional coverages of each PFT using the old and new methods for calculating surface vegetation are shown in Table 1. The fractional coverages shown are for a T42-resolution global grid. The bare soil fraction is doubled from 0.174 to 0.352 because of the inclusion of FVC. This new global bare soil fraction in the model is close to the global nonvegetated fraction of 0.321 calculated from Table 1 of Zeng et al. (2000). Tree PFTs show little change in fractional coverage, as expected. The increase in bare soil in the new dataset comes mainly from decreases in fractional coverage of shrubs (35%–67% decrease), grass (18%–21% decrease), and crop (13% decrease). In particular, the current FVC for the deciduous broadleaf temperate shrub (PFT 10) is reduced by a factor of 3. Figure 3 also shows that this specific shrub is reduced by up to 0.4 in FVC in central Australia.

#### c. Modeling methods

To assess how the addition of FVC is affecting the CAM2/CLM2 modeling system, 22-yr simulations are

TABLE 2. Regional changes in bare soil fraction from the current and new method of PFT calculation for several global latitude and longitude ranges.

Region	Lat range	Lon range	Current	New
Alaska/northwest Canada	50°–70°N	170°–100°W	0.154	0.338
Northern Europe	55°–70°N	5°–60°E	0.018	0.096
Western Siberia	50°–70°N	60°–90°E	0.012	0.127
Eastern Siberia	50°–70°N	90°–140°E	0.016	0.138
Western United States	30°–50°N	130°–110°W	0.007	0.329
Central United States	30°–50°N	110°–90°W	0.000	0.192
Eastern United States	30°–50°N	90°–70°W	0.000	0.015
Central Europe	40°–55°N	10°W–40°E	0.000	0.114
Central America	10°–25°N	110°–80°W	0.000	0.069
Amazon	10°S–0°	70°–50°W	0.000	0.024
Congo	10°S–5°N	10°–30°E	0.001	0.047
India	10°–30°N	70°–90°E	0.034	0.320
Sahara	10°–30°N	20°W–50°E	0.679	0.816
Southern South America	60°–25°S	80°–50°W	0.071	0.304
Southern Africa	35°–10°S	10°–40°E	0.063	0.291
Australia	40°–10°S	110°–160°E	0.002	0.408

completed using three different land surface specifications. The control simulation (CNTL) is run with an unadulterated version of the model. Second, a simulation (PFT/OLDLAI) with just the new PFT changes is completed.

Vegetation amount is computed as FVC multiplied by LAI with respect to vegetated area. To maintain a constant vegetation amount, LAI needs to be rescaled based on  $LAI_{new} \times FVC_{new} = LAI_{old} \times FVC_{old}$  if FVC is adjusted. Limitations are set so the LAI for any PFT cannot exceed the current global maximum for that PFT. After this global rescaling, a third simulation (PFT/NEWLAI) is completed. The only difference between PFT/OLDLAI and PFT/NEWLAI is the value for each grid's LAI. The rescaling is necessary because vegetation amount is derived from satellite reflectance, which should remain constant. Completion of both PFT/OLDLAI and PFT/NEWLAI allows for the testing of the sensitivity to the necessary adjusting of LAI.

The simulations are run using the CAM2/CLM2 system running at T42 (approximately 2.8°) horizontal resolution with 26 unevenly spaced vertical levels. The CAM2 atmospheric model parameterizes deep convection, shallow and nonprecipitating convection, short-wave and longwave radiation, large-scale precipitation, and atmospheric turbulence. Observed monthly sea surface temperatures and sea ice coverage are prescribed in these simulations. The model operates on a 20-min time step for all processes except radiation, which is calculated every 60 min. Additional model details are provided in Collins et al. (2003).

The climatology simulations (CNTL, PFT/OLDLAI, and PFT/NEWLAI) start from 1 September 1979 and end on 31 December 2000. The land surface begins with an arbitrary initialization. Only the final 20 years (1981–2000) are analyzed for the climatology results.

### 3. Results

Figure 4 shows the control simulation seasonal surface air temperature bias compared to Willmott and Mat-

suura (2000) observations for the four seasons. Monthly surface air temperature in the model is an average over all time steps while for the observations, the climatological average is comprised of the mean of daily minimum and maximum temperatures. Although some differences may result from the different methods of calculating monthly air temperature, it is the only way to provide continuity with the previous results of Bonan et al. (2002b). For each month, the climatological average is calculated by taking the mean of the 20 occurrences of that month in the 20-yr simulation. In comparison to Fig. 7 of Bonan et al. (2002b), where an earlier version of CAM2 was used, the results are very similar. Regions of positive and negative bias remain in the same locations. Although some regions show improvement and some degradation, the use of the newer version of CAM2 seems to have little effect on the surface air temperature compared to the older version, except to possibly strengthen the northern high-latitude warm bias.

The global effects of the new PFT and rescaled LAI compared to the control simulation for 2-m air temperature are shown in Fig. 5. Temperature at 2 m is a widely measured surface state variable with a long record and is used here to test model improvement. Locations where differences are statistically significant with a 95% confidence based on a Student's *t* test are shown with stippling. The differences are consistent over several sparsely vegetated regions such as Australia, southern South America, the southwestern United States, the Sahel, and the Himalayas. Many other regions in the northern high latitudes and the Arabian Peninsula also show substantial changes in more than one season. Most of the statistically significant changes occur in the regions where shrub or grass is replaced by bare soil (see Fig. 3). The decreases in 2-m temperature for these regions are typically on the order of 1–2 K. Most of these changes reduce the model bias in these regions, especially in the summer for midlatitudes and winter for northern high latitudes.

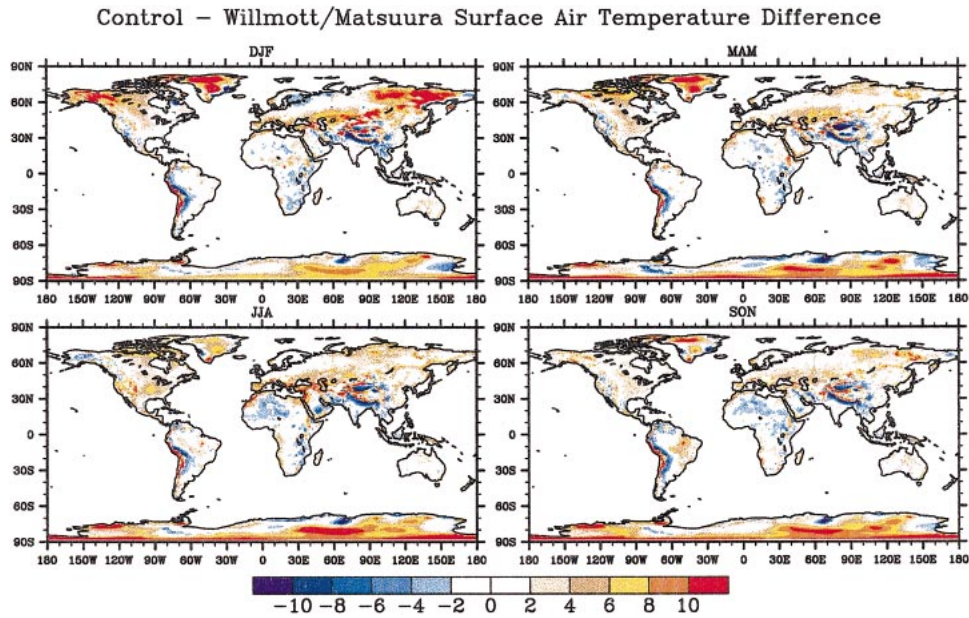


FIG. 4. CAM2/CLM2 control simulation 2-m air temperature bias (K) (model – observations) over land compared to Willmott and Matsuura (2000) observations for the four seasons [Dec–Feb (DJF), Mar–May (MAM), Jun–Aug (JJA), and Sep–Nov (SON)]. Model temperature is averaged over all time steps, while observed mean temperature is the average of daily minimum and maximum temperatures.

A variable like 2-m temperature is not representative of the most dramatic changes that will occur when vegetation is replaced by bare soil. Ground temperature is much more strongly affected by the new method of PFT calculation because of its more immediate role in the surface energy budget. For instance, the arid and semi-

arid regions with bare soil fraction increase in Fig. 3 show a statistically significant decrease in ground temperature by up to 10 K throughout the year (Fig. 6). The warm bias in ground temperature in the control simulation is primarily caused by the inadequate representation of undercanopy turbulence for thin canopies

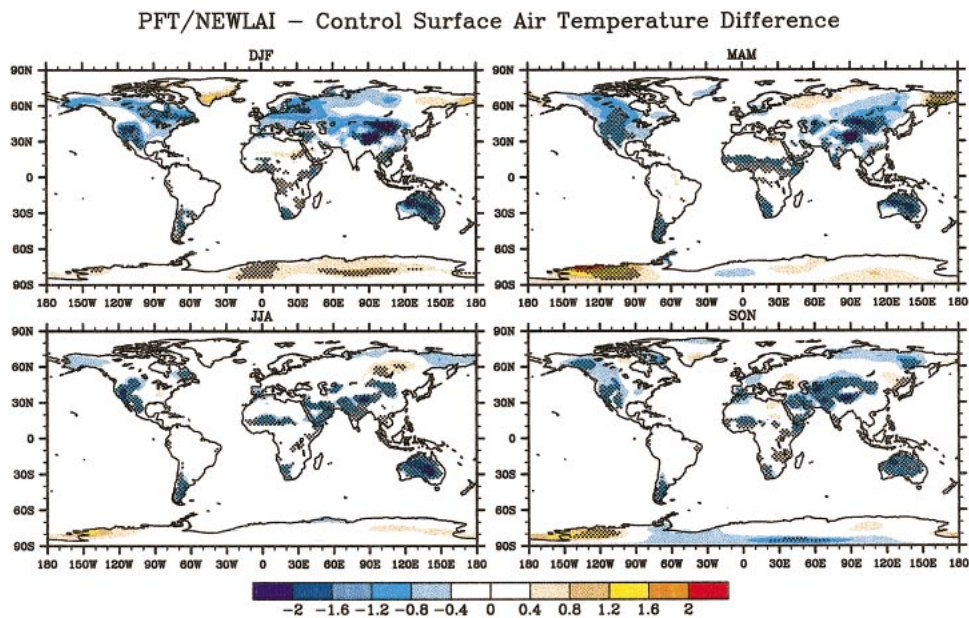


FIG. 5. Two-meter air temperature difference (K) between the CAM2/CLM2 control simulation and the new PFT simulation with rescaled LAI for the four seasons (DJF, MAM, JJA, and SON). Stippling indicates statistically significant differences at the 95% level.

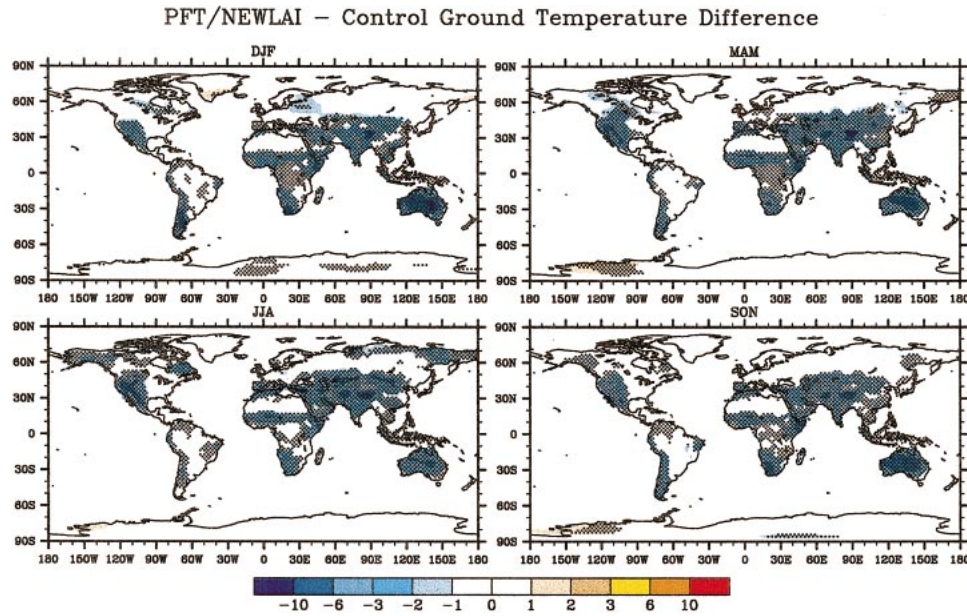


FIG. 6. Ground temperature difference (K) between the CAM2/CLM2 control simulation and the new PFT simulation with rescaled LAI for the four seasons (DJF, MAM, JJA, and SON). Stippling indicates statistically significant differences at the 95% level.

(e.g., over arid regions; Zeng et al. 2004, manuscript submitted to *J. Climate*). The increase of bare soil fraction in the FVC data essentially decreases the fraction of thin canopy in a grid cell that is affected by this model deficiency. For large-scale variables, such as precipitation and runoff, that are more nonlinearly related to local changes in bare soil coverage, several large

changes exist over some regions, but the relationship does not appear to be statistically significant (figures not shown).

Figure 7 shows the monthly 2-m air temperature bias from Willmott and Matsuura (2000) observations averaged over Australia (see Table 2 for latitude and longitude ranges) for the three simulations. Australia was chosen for analysis because its PFTs are strongly affected by the FVC additions and it shows model bias improvement. Results are similar for other sparsely covered regions. The bias of 2-m air temperature decreases with the new FVC addition in every month except January. The PFT/NEWLAI simulation has slightly lower temperatures probably due to extra transpiration from increased LAI resulting from the rescaling of shrub and due to the undercanopy turbulence issue discussed earlier.

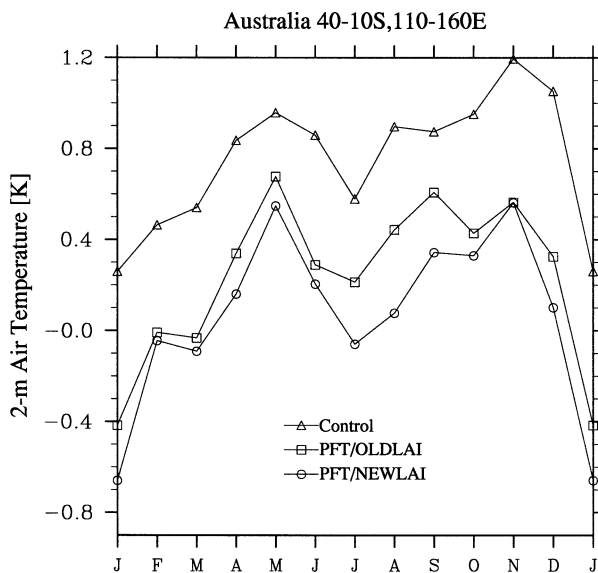


FIG. 7. Monthly bias of 2-m air temperature (K) in Australia relative to observations for the control (triangle), new PFT with unchanged LAI (squares), and new PFT with rescaled LAI (circles) simulations. Each data point is an average of all land points in the region defined as Australia in Table 2.

The effects that the PFT/OLDLAI and PFT/NEWLAI changes have on the surface energy budget relative to the control simulation are shown in Fig. 8 for the Australia region. The large decrease of ground temperature in the PFT/NEWLAI simulations (see Fig. 6) results in an increase in net longwave radiation absorbed by the surface. This is balanced primarily by the decrease of absorbed solar radiation due to the higher albedo of bare soil relative to that of shrubs and the increase in both sensible and latent heat fluxes. The variation in ground heat flux is relatively small compared with the above terms. Increases in ground evaporation from the decrease in overlying canopy account for most of the changes to latent heat flux. These increases are mitigated slightly by a decrease in canopy evaporation in the austral summer.

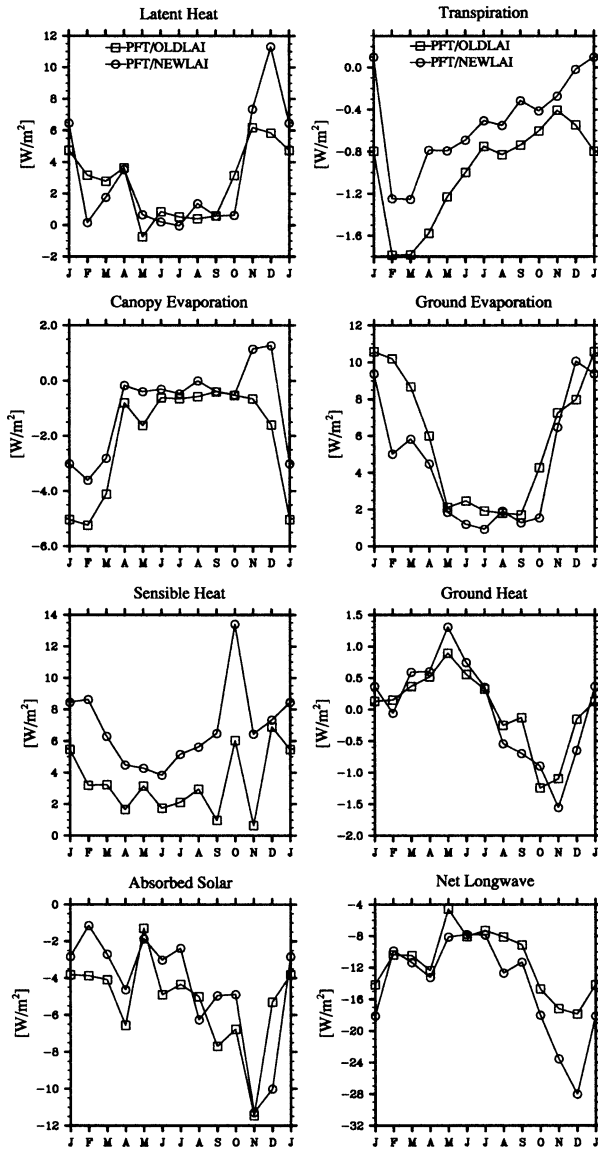


FIG. 8. Regionally averaged mean annual cycle of surface energy flux differences ( $W m^{-2}$ ) in Australia relative to the control simulation for the new PFT with unchanged LAI (squares) and new PFT with rescaled LAI (circles) simulations. Latent heat is the sum of transpiration, canopy evaporation, and ground evaporation. Negative net longwave implies surface energy gain from the atmosphere.

A similar pattern is found in other shrub-covered mid-latitude regions. In high-latitude shrub regions in winter, increases in bare soil fraction and subsequent decreases in canopy coverage significantly increase albedo because of more complete snow coverage, decreased surface available energy, and decreased temperature.

**4. Summary**

The current surface cover in CLM2 contains too little bare soil in sparsely vegetated areas because the current method of generating PFT coverage will contain bare

soil only if bare soil is the dominant IBGP land cover type and is one of the four most prevalent when scaled to the model grid. Using an approach similar to Bonan et al. (2002a), a new fractional vegetation cover database is used to determine a new PFT coverage. Regions with large tree coverage and regions with no vegetation are not affected. Regions with sparse vegetation are the most highly affected by the inclusion of the FVC data with fractional shrub coverage decreasing up to 0.4 in central Australia.

The global bare soil fraction in CLM2 increases from 0.174 to 0.352 because of the inclusion of FVC, which is close to the global nonvegetated fraction of 0.321 calculated from Zeng et al. (2000). Smaller changes occur for tree PFTs with increasing changes for crop (13% decrease in FVC), grass (18%–21% decrease in FVC), and shrubs (35%–67% decrease in FVC). Shrub- and grass-dominated regions, such as the western United States, southern South America, and southern Africa, show large increases in bare soil. The largest changes occur in Australia, with an increase of over 0.4 in bare soil fraction.

The control simulation seasonal 2-m air temperature bias compared to observations for the four seasons is very similar to the Bonan et al. (2002b) climatology where the earlier version of CAM2 is used. The global effects of the new PFT and rescaled LAI compared to the control simulation for 2-m air temperature show statistically significant differences over several regions such as Australia, southern South America, the southwestern United States, the Sahel, and the Himalayas. Many other regions in the northern high latitudes and the Arabian Peninsula also show substantial changes in more than one season. Most of the statistically significant changes occur in the regions where shrub or grass is replaced by bare soil. The decreases in 2-m temperature for these regions are typically on the order of 1–2 K and reduce discrepancy between model results and observations, especially in the summer for midlatitudes and winter for northern high latitudes.

Ground temperature is much more strongly affected by the new method of PFT calculation and shows a statistically significant decrease in ground temperature by up to 10 K throughout the year over arid and semiarid regions. Other large-scale variables, such as precipitation and runoff, show only slight statistically significant relationships.

At the regional scale, the monthly 2-m air temperature bias over Australia decreases with the new FVC addition in nearly every month. This results in an increase in net downward longwave radiation, which is balanced by the increase of latent and sensible heat fluxes and the decrease of absorbed solar radiation. The increases in latent and sensible heat are of similar magnitude. Increases in ground evaporation account for most of the changes to latent heat flux.

Modeling results show that the CAM2/CLM2 system is sensitive to the inclusion of FVC in the PFT coverage

map when analyzing the surface energy budget and surface temperature. One of the limitations of the current version of CAM2/CLM2 is that PFT coverages are not allowed to change interannually. This will change in the future as dynamical vegetation models are incorporated into the CAM2/CLM2 system. This study shows that high model sensitivity in the surface energy budget can occur in semiarid regions, which can have high interannual variability in bare soil fraction (see Zeng et al. 2003). This sensitivity implies that care must be taken to provide accurate input datasets. As more accurate and higher resolution datasets derived from satellite or in situ measurements inevitably become available, the methodology of this study is adaptable to these new data. Similarly, the data-generating methodology can also be applied easily to other land models.

*Acknowledgments.* This work was supported by NOAA under Grant NA06GP0569 and NASA under Grant NAG5-13322 and through its EOS IDS Program (429-81-22). The authors would like to thank the three anonymous reviewers for several insightful, detailed suggestions that improved the final version substantially.

#### REFERENCES

- Bonan, G. B., S. Levis, L. Kergoat, and K. W. Oleson, 2002a: Landscapes as patches of plant functional types: An integrating concept for climate and ecosystem models. *Global Biogeochem. Cycles*, **16**, 1021, doi:10.1029/2000GB001360.
- , K. W. Oleson, M. Vertenstein, S. Levis, X. Zeng, Y. Dai, R. E. Dickinson, and Z.-L. Yang, 2002b: The land surface climatology of the Community Land Model coupled to the NCAR Community Atmosphere Model. *J. Climate*, **15**, 3123–3149.
- Collins, W. D., and Coauthors, cited 2003: Description of the NCAR Community Atmospheric Model (CAM). [Available online at <http://www.cesm.ucar.edu/models/atm-cam/docs/description/index.html>.]
- Dai, Y., and Coauthors, 2003: The common land model. *Int. J. Climatol.*, **84**, 1013–1023.
- DeFries, R. S., J. Townshend, and M. C. Hansen, 1999: Continuous fields of vegetation characteristics at the global scale at 1-km resolution. *J. Geophys. Res.*, **104D**, 16 911–16 923.
- , M. C. Hansen, J. Townshend, A. C. Janetos, and T. Loveland, 2000: A new global 1-km dataset of percentage tree cover derived from remote sensing. *Global Change Biol.*, **6**, 247–254.
- Legates, D. R., and C. J. Willmott, 1990a: Mean seasonal and spatial variability in gauge-corrected, global precipitation. *Int. J. Climatol.*, **10**, 111–127.
- , and —, 1990b: Mean seasonal and spatial variability in global surface air temperature. *Theor. Appl. Climatol.*, **41**, 11–21.
- Loveland, T., B. C. Reed, J. F. Brown, D. O. Ohlen, Z. Zhu, L. Yang, and J. W. Merchant, 2000: Development of a global land cover characteristics database and IGBP DISCOVER from 1km AVHRR data. *Int. J. Remote Sens.*, **21**, 1303–1330.
- Willmott, C. J., and K. Matsuura, cited 2000: Terrestrial air temperature and precipitation: Monthly and annual time series (1950–1996). [Available online at [http://climate.geog.udel.edu/~climate/html\\_pages/README ghen\\_ts2.html](http://climate.geog.udel.edu/~climate/html_pages/README ghen_ts2.html).]
- Zeng, X., R. E. Dickinson, A. Walker, M. Shaikh, R. S. DeFries, and J. Qi, 2000: Derivation and evaluation of global 1-km fractional vegetation cover data for land modeling. *J. Appl. Meteor.*, **39**, 826–839.
- , M. Shaikh, Y. Dai, R. E. Dickinson, and R. Myneni, 2002: Coupling of the common land model to the NCAR community climate model. *J. Climate*, **15**, 1832–1854.
- , P. Rao, R. S. DeFries, and M. C. Hansen, 2003: Interannual variability of global fractional vegetation cover from 1982 to 2000. *J. Appl. Meteor.*, **42**, 1525–1530.